Mathematics Interdisciplinary Research **10** (1) (2025) 71 − 94

Original Scientific Paper

Control and Synchronization of a Chaotic Memristor System Based on Graphical Approach

*Marzieh Pabasteh and Bashir Naderi**

Abstract

In this article, we analyze a four-dimensional chaotic system, focusing on bifurcation and the Lyapunov exponent as key characteristics under new parameter settings. Our main goal is to control the system using a graphical algorithm based on contraction method in dynamical systems. The controller designed using this method is simpler than most controllers for chaotic systems. Since chaotic systems are sensitive to initial conditions, their synchronization and control are essential challenges. The graphic algorithm is used for both controlling and synchronizing the chaotic memristor system. Also, we utilize the synchronization results for secure communication, employing master and slave systems as encryption and decryption keys. The effectiveness of the proposed method is demonstrated through numerical simulations.

Keywords: Contraction theory, Chaos, Secure communication, Graphical approach, Synchronization.

2020 Mathematics Subject Classification: 65L05, 34K06, 34K28.

How to cite this article
M. Pabasteh and B. Naderi, Control and synchronization of a chaotic memristor system based on graphical approach, *Math. Interdisc. Res.* **10** (1) (2025) 71-94.

*Corresponding author (E-mail: b_naderi@pnu.ac.ir)
Academic Editor: Abbas Saadatmandi
Received 9 June 2024, Accepted 3 December 2024
DOI: 10.22052/MIR.2024.255020.1468

© 2025 University of Kashan
This work is licensed under the Creative Commons Attribution 4.0 International License.

1. Definitions and notations

Chaos is a concept often used for a nonlinear dynamic. Chaos theory is a mathematical tool that extracts beautiful structures from chaos. The origins of chaos theory were introduced by Henri Poincaré in 1908, who attempted to study an unsolved problem of Newtonian Laplacian celestial mechanics (the three-body problem). During this research, Poincaré realized that infinitely complex behavior may exist in nonlinear systems. Chaos theory was first discussed by MIT meteorologist Edward Lorenz, who simulated weather patterns on computers in the 1960 [1]. In recent years, deterministic chaos has been seen as a model in electronic circuits, laser technology, cardiology, organizations, financial markets, urban communities, and climate.

Managing and directing chaos is a crucial aspect of our daily routine. To achieve desired outcomes, it is necessary to control various chaos systems. The Lyapunov theory has been the basis for controlling most chaotic systems, including the Chen turbulence system, the Duffing system, and the Genesio-Tesi system [2–8]. However, a new technique known as contraction has emerged as a viable alternative to prior stability analysis methods. This method, introduced by Slotine [9, 10], differs because it does not rely on Lyapunov's function.

Despite their strong dependence on initial conditions, chaotic systems can achieve synchronization. In 1990, Carroll and Pecora first investigated the synchronization of two chaotic systems, which has since garnered attention for its potential use in secure communication [11]. To synchronize and control chaotic systems, researchers have utilized various methods such as adaptive control, OGY method, feedback controller, and observer-based control. Despite their complexity, these methods rely on Lyapunov stability analysis and the linear matrix inequality approach to ensure asymptotic synchronization [8, 12–17].

A novel technique called contraction analysis draws inspiration from fluid mechanics to study the convergence of nonlinear systems. According to this method, a system is deemed stable if its behavior remains unaffected by initial conditions. A shrinking system is one where paths converge on each other. By applying the contraction method, we can determine the controller and synchronization of chaotic systems. The beauty of this approach lies in its ability to generate a linear controller for intricate systems.

In 1971 Leon Chua, introduced the fourth circuit element in the concept of a memristor [18]. In 2008, the Stanley Williams Group of Hewlett-Packard (HP) announced the first solid-state implementation of a memristor [19]. After that, the researchers, because they wanted to replace the Chua diode system of the Chua circuit, focused on building different memristor-based chaotic circuits and then completing the dynamic analysis. In 2011, Corintoise discovered a chaotic oscillator containing three flux-controlled memristors through coupling [20]. In 2013, Lee proposed a memristor oscillator based on a Twin-T network [21]. The inherent nonlinearity of memristors has caused the nonlinear resistance in classic chaotic, circuits to be replaced with memristors for the design of new chaotic

circuits, and this has caused us to have a rich set of nonlinear behaviors [22–24]. Because mathematical models and designed circuit of memristor cannot be used in physical applicable problems, active memristor simulator circuits with the same dynamic behavior as TiO2 memristor have started to work in the literature. Recently, many simulator circuits have been implemented [25]. In 2020, a memristor simulator model was introduced in the article, which allows the implementation of other sets of chaotic equations [26]. Recently, due to the importance and interesting features of the memristor system, this system has received more attention. For example, the authors of [27] discuss the principles of whether nonlinear systems with memristor functionality can be realized using memristor devices. Recently, the use of a chaotic oscillator with a memristor to generate chaos with minimum nonlinearity is discussed; and a new multistage chaotic system with a memristor and mem capacitor for fractional order is made [28, 29].

According to what has been mentioned and considering the benefits of contraction and graphical methods, this article introduces a control approach for dynamic systems utilizing a graphic algorithm based on the contraction method. The proposed method is applied in the synchronization of chaotic systems. Furthermore, the obtained synchronization results are utilized for secure communication, employing a master-slave system for encryption and decryption.

The article follows these sections: Section 2, explains the contraction method and graphical method of contraction. Section 3, introduces the four-dimensional circuit dynamic system based on a memristor. Section 4, describes and discusses the control and synchronization of the four-dimensional circuit dynamic system based on a memristor. In Section 5, secure communication is reviewed, and in Section 6, security analysis is done. Finally, Section 7, concludes the article.

2. Contraction and graphical system

In this section, we will discuss the notion of contraction and subsequently elaborate on the graphical algorithm employed to demonstrate contraction.

2.1 Basics of contraction theory

For analyzing the behavior of state variables in a nonlinear system, the contraction theory is used as a tool, such that paths towards each other in the form of state space [9, 30]. If we consider two arbitrary paths, in this theory, these two paths converge and are a so-called nonlinear dynamic system. We will have contraction. For more details, We state some basic definitions and results of the contraction theory. For this aim, consider the following nonlinear system:

$$\dot{x} = f(x, t), \tag{1}$$

where $x \in R^{m\times 1}$ is the state vector of the dynamical system (1) and f is a continuous and differentiable vector function. Let δx be the virtual displacement

in the state x, which refers to infinitesimal displacements at a fixed time. The concept of virtual dynamics, based on (1) is defined as follows:

$$\delta\dot{x} = \frac{\partial f\,(x,t)}{\partial x}\delta x, \tag{2}$$

By considering this equation, we have:

$$\frac{d}{dt}\left(\delta x^T \delta x\right) = 2\delta x^T \delta\dot{x} = 2\delta x^T \frac{\partial f}{\partial x}\delta x \leq 2\lambda_m\,(x,\ t)\,\delta x^T \delta x. \tag{3}$$

Here, the Jacobian matrix is denoted as $J = \frac{\partial f}{\partial x}$ and $\lambda_m\,(x,\ t)$ is the largest eigenvalue of the symmetric part of the matrix J. If the eigenvalue $\lambda_m\,(x,t)$ is strictly uniformly negative, and $\delta x^T \delta x$ represents the distance between the neighboring trajectories, then any minimal length of $\|\delta x\|$ converges to zero exponentially. By considering the path integration in (2), it can be inferred that all the system trajectories in(1) converge to the same trajectory exponentially.

Definition 2.1. Let $\dot{x} = f\,(x,t)$ be a dynamical system. If the Jacobian matrix $J = \frac{\partial f}{\partial x}$ is uniformly negative definite (UND) in a region, then the variables of state space are called contracting in the region.

Definition 2.2. The Jacobian matrix $J = \frac{\partial f(x,\,t)}{\partial x}$ if UND, if there exists a scalar $\beta > 0$, for all x and $t \geq 0$ such that $\frac{\partial f}{\partial x} \leq -\beta I < 0$.

So, $\frac{1}{2}\left(\frac{\partial f}{\partial x} + \frac{\partial f^T}{\partial x}\right) \leq -\beta I$ is negative definite [16, 31, 32]. According to the above definition, in the following theorem, the convergence of two different paths in the contraction area is obtained [33]:

Theorem 2.3. *([33]). Let C be a convex subset of R^m, and let $f\,(t,x)$ be infinitesimally contracting with contraction rate c^2. Then, for any two solutions $x(t) = \varphi\,(t,0,\xi)$ and $z(t) = \varphi\,(t,0,\zeta)$, the following holds:*

$$|\ x(t) - z(t)\ | \leq e^{-c^2 t}\ |\ \xi - \zeta\ |, \qquad \forall t \geq 0. \tag{4}$$

In other words, infinitesimal contractility implies global contractility. According to the above definitions and theorem, the main results (without proof) related to the exponential convergence of paths can be stated as follows:

Lemma 2.4. *Let the dynamical system be given as $\dot{x} = f\,(x,t)$, any trajectory that begins within a fixed radius ball centered on a specific trajectory and stays within a contraction region will stay in that ball and will converge to the given trajectory. Moreover, if the whole state space region is contracting, then guaranteed the global exponential convergence to this trajectory.*

To explore the concepts mentioned above, we introduce a coordinate transformation defined by:

$$\delta z = \theta \delta x, \tag{5}$$

Here, $\theta(x,t)$ signifies a uniformly invertible matrix. For detailed definitions and theorems in the extended domain, refer to [31, 32, 34]. In certain systems described by the representation in (1), the Jacobian matrix $\frac{\partial f}{\partial x}$ could be characterized as negative semi-definite. These systems are called semi-contracting systems, building upon the extension of definition (2.1). Consequently, utilizing contraction theory, outcomes can guarantee asymptotic stability for such systems.

2.2 Graphical approach

In this section, a graphical method is considered to check the system contraction. In this method, non-Euclidean norms and matrix criteria are used to analyze nonlinear dynamic systems. With this approach, we can graphically determine whether a system is contracting. This is super useful for designing control strategies to shrink a system or achieve consensus and synchronization among a network of nonlinear oscillators. One notable aspect of this method is that there is no need to identify a specific metric to which all trajectories converge. Instead, we focus on establishing sufficient conditions for the existence of such a metric. This expands the range of systems to which contraction analysis can be quickly and successfully applied. According to the discussed topics, this algorithm can be used to design a controller or synchronization in a network of nonlinear oscillators. This algorithm was obtained in [11, 35, 36].

Theorem 2.5. *([37, 38]). The continuous-time dynamical system* $\dot{x} = f(x,t)$, $(R^{m\times 1})$ *is contracting, if its Jacobian matrix,* J*, is satisfied in the following conditions:*

- $J_{ii}(t,x) < 0$*, for all* $i = 1,\ldots,m$*.*
- *The graph* $G_d(A)$ *constructed from* J *as detailed above does not contain (directed) loops and* $\beta_{ij}(t,x)\,\beta_{ji} \leq 1$*.*

From the above theorem, we have the following algorithm for the continuous state system:

2.2.1 Graphical algorithm

The steps of the graphical algorithm are as follows:
Step 1: Obtain the Jacobian matrix of the given system, which is generally state and time-dependent.

$$J = \frac{\partial f(x,\,t)}{\partial x} = \begin{pmatrix} J_{1,1} & J_{1,2} & \cdots & J_{1,m} \\ J_{2,1} & J_{2,2} & \cdots & J_{2,m} \\ \vdots & \vdots & \ddots & \vdots \\ J_{m,1} & J_{m,2} & \cdots & J_{m,m} \end{pmatrix}. \tag{6}$$

Step 2: Construct a directed graph for the Jacobian system. To build this graph, it is necessary to build the adjacency matrix A with the following conditions:

- initialize A so that $a_{ij} = 0$, for all i, j,
- for all $i \neq j$, set $a_{ij} = a_{ji} = 1$ if either $J_{i,j}(t,x) \neq 0$, or $J_{j,i}(t,x) \neq 0$.

So far, we have a graph $G(A)$ in which the connection between the vertices is defined, but its direction is not yet defined [39].
Step 3: Find a directed graph $G_d(A)$ of $G(A)$. For this purpose, we consider the following relationship:

$$\alpha_{ij}\,(t,x) = \frac{\mid J_{i,j}(t,x)\mid}{\mid J_{i,i}(t,x)\mid}(m - n_{0i} - 1). \tag{7}$$

Where n_{0i} is the number of zeros in the i-th row of matrix A. In calculating aij, we must ensure that $Ji,i(t,x)$ is not equal to zero. If $Ji,i(t,x)$ is zero, it is necessary to manage the structure such that all system parameters $Ji,i(t,x)$ are non-zero before calculating (7).
After obtaining α_{ij}, we determine the direction using the following rule:

- if $\alpha_{ij}(t,x) < 1$ then directed from i to j,
- if $\alpha_{ij}(t,x) \geq 1$ then directed from j to i.

Since s is time-dependent, the directions of the graph may change over time. Therefore, because the direction can change, the connection between nodes i and j is bidirectional.
After the mentioned steps, contraction is guaranteed under the following conditions:

- All elements on the main diagonal of the Jacobian matrix must be negative, which means $J_{i,i}(t,x) < 0$, $\forall\, i$.
- There are no loops in a directed graph for all t.
- for any $i \neq j$, $\alpha_{ij}(t,x)\alpha_{ji}(t,x) \leq 1$.

Note that when the conditions mentioned above are not satisfied, we can impose a contraction on the system in the following manner:

- If possible, a control input should be applied to the system so that the elements on the primary diameter are all negative.
- If possible, a control input should be applied to the system so that the directions are such that they do not form a loop.
- The direction of the edges between two nodes i, and j should satisfy one of the following conditions:

– if $\alpha_{ij}(t,x) < 1$ then directed from i to j,
– if $\alpha_{ij}(t,x) \geq 1$ then directed from j to i,
– be sure that $\alpha_{ij}(t,x)\alpha_{ji}(t,x) \leq 1$.

Because our system is continuous time, we expressed all the steps of the algorithm in this way. For a discrete-time, you can refer to [6, 37].

3. The memristor-based four-dimensional system

The concept of memristor as the fourth circuit element was introduced by Leon Chua back in 1971 [18]. In 2008, the Hewlett Packard (HP) Group under Stanley Williams announced the first solid-state implementation of the memristor [19]. However, due to its physical and mathematical complexity, a memristor simulator model was developed in 2020 to facilitate the implementation of other sets of chaotic equations [26]. The mathematical model of the system is defined as follows:

$$\begin{cases} \dot{x_1}(t) = a_1 p_1 x_1(t) - a_1 x_3(t) - a_1 p_2 x_1(t) x_4^2(t), \\ \dot{x_2}(t) = -a_2 x_3(t), \\ \dot{x_3}(t) = -a_3(x_1(t) - x_2(t)), \\ \dot{x_4}(t) = -a_4 x_1(t). \end{cases} \tag{8}$$

Where x_1, x_2, x_3, x_4 are state variables and $a_1 = 3.75, a_2 = 10, a_3 = 1, a_4 = 1, p_1 = 0.33, p_2 = 0.25$ are the constant parameters of the system. At these specific parameter values the system is chaotic. Now, we disscuss the behavior of system (8) for new parameters. For more details, we will examine attractor, sensitivity, Lyapunov view, and bifurcation of system (8).

3.1 Attractor and sensivity

An attractor denotes a collection of points that gravitate towards the system's orbit as the iteration count increases, essentially representing a stable solution (equilibrium) towards which the system tends. When trajectories originating from very similar initial conditions separate quickly, leading to entirely different future states, it demonstrates that the sensitivity of the chaotic system is dependent on initial conditions. Sensitivity is a show of chaos and a fundamental characteristic of chaotic systems. Because initial conditions cannot be measured or specified with infinite precision, sensitivity to initial conditions in chaotic systems makes short-term prediction impossible. The outcomes are illustrated in Figures 1 to 4.

3.2. Lyapunov exponent

Lyapunov's view determines the stability or instability of a system. Lyapunov's exponent determines how fast a minimal distance between two states that were

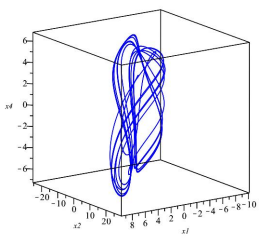
$a_2 = 10.5$, $a_4 = 0.5$

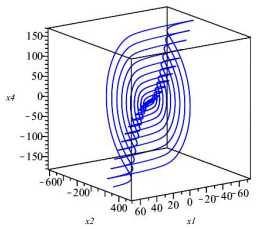
$a_2 = 12$, $a_4 = 1.5$

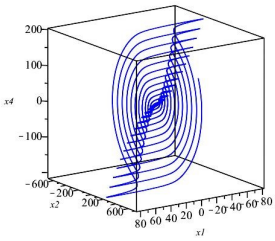
$a_4 = 1.5$,$a_2 = 10.5$

Figure 1: Attractors of system (8) for $a_1 = 3.75$, $a_3 = 1$, $p_1 = 0.33$, $p_2 = 0.25$.

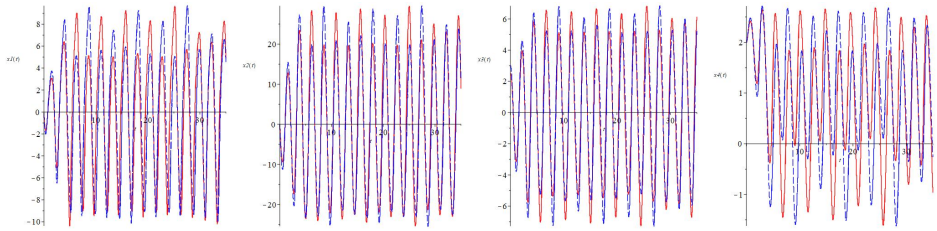

Figure 2: Sensitivity for $a_4 = 0.5$ for initial conditions $(-0.1, 0, 3, 2)$ and $(-0.1, 0, 2.5, 2)$.

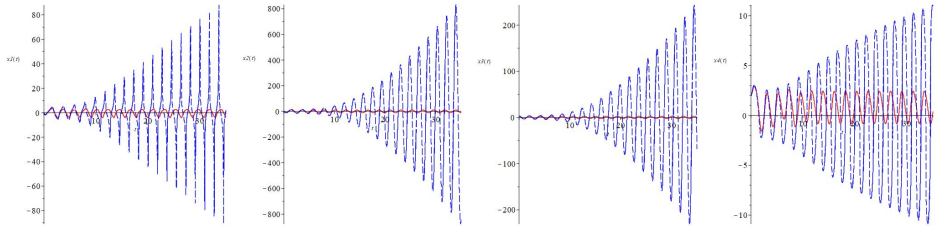

Figure 3: Sensitivity for $a_2 = 12$ for initial conditions $(-0.1, 0, 3, 2)$ and $(-0.1, 0, 2.5, 2)$.

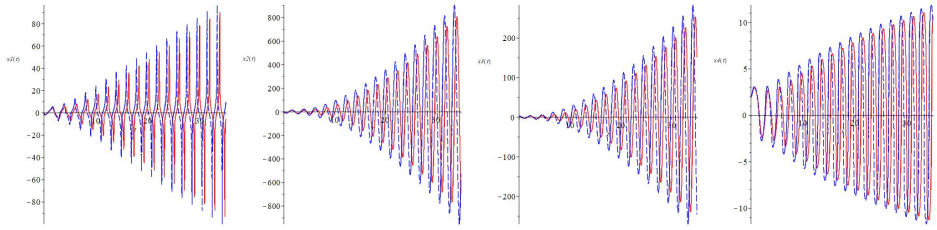

Figure 4: Sensitivity for $a_2 = 10.5, a_4 = 0.5$ for initial conditions $(-0.1, 0, 3, 2)$ and $(-0.1, 0, 2.5, 2)$.

initially closed grows over time. For this, the following formula is used:

$$F^t(x_0+\epsilon) - F^t(x_0) \approx \epsilon e^{\lambda t}, \tag{9}$$

amount of power λ over a long period of time (ideally $t \to \infty$) is measured and it is the Lyapunov exponent. When λ is greater than zero, short distances steadily increase over time, indicating that the stretching mechanism is active. Conversely, when λ is less than zero, shorter distances do not continually increase, signifying that the system ultimately settles into a periodic trajectory [40]. Here, we plot the Lyapunov exponent for the system (8) for the given values and initial conditions. Figures 5 and 6 show the results.

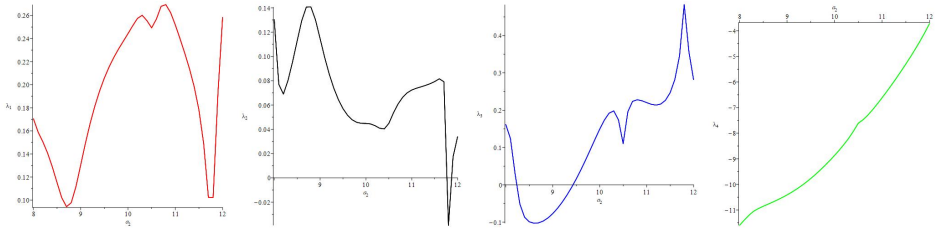

Figure 5: Lyaponuv exponent of system (8) for $p_1 = 0.33$, $p_2 = 0.25$, $a_1 = 3.75$, $a_3 = 1$, $a_4 = 1.5$ and $8 \leq a_2 \leq 12$.

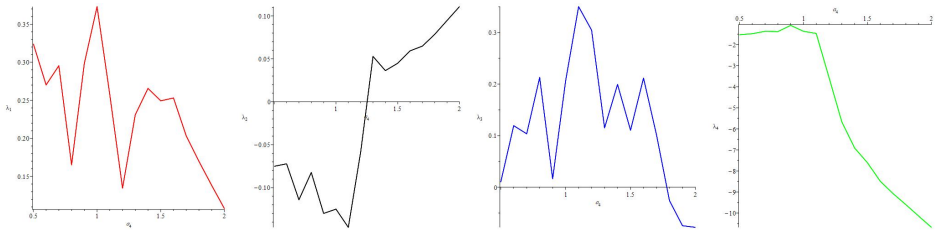

Figure 6: Lyaponuv exponent of system (8) for $p_1 = 0.33$, $p_2 = 0.25$, $a_1 = 3.75$, $a_2 = 10.5$, $a_3 = 1$ and $0.5 \leq a_4 \leq 2$.

3.3. Bifurcations

Bifurcation signifies a fundamental change in the behavior of a dynamic system by adjustments in a system parameter. A bifurcation chart illustrates the potential long-term outcomes of a system variable concerning a system parameter. Now, we draw the bifurcation for the system (8) for the given values and initial conditions. Figures 7 and 8 show the bifurcation results.

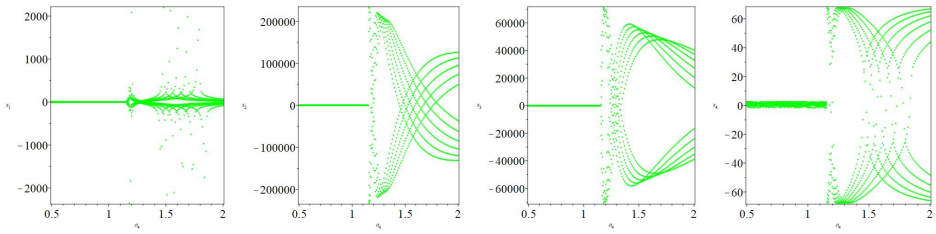

Figure 7: Bifurcation diagram of system (8) for $p_1 = 0.33$, $p_2 = 0.25$, $a_1 = 3.75$, $a_2 = 10.5$, $a_3 = 1$ and $0.5 \leq a_4 \leq 2$.

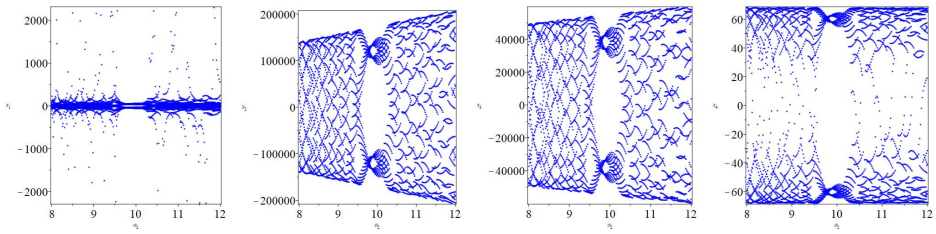

Figure 8: Bifurcation diagram of system (8) for $p_1 = 0.33$, $p_2 = 0.25$, $a_1 = 3.75$, $a_3 = 1$, $a_4 = 1.5$ and $8 \leq a_2 \leq 12$.

4. Control and synchronization of memristor chaotic system

According to the control method proposed in subsection 2.2, in this section we want to apply the results on the system (8), and we also study the synchronization of the system (8).

4.1 Control

In Section 3, it is evident that system (8) operates chaotically. Thus, it is imperative to develop a controller for the system. To identify the appropriate controller, we employ the graphical contraction control technique. The first step in this algorithm involves obtaining the Jacobian matrix of system (8).

$$J = \begin{pmatrix} a_1 p_1 - a_1 p_2 x_4^2 & 0 & -a_1 & -2a_1 p_2 x_1 x_4 \\ 0 & 0 & -a_2 & 0 \\ -a_3 & a_3 & 0 & 0 \\ -a_4 & 0 & 0 & 0 \end{pmatrix}, \tag{10}$$

We can create the adjacency matrix A by using the Jacobian matrix.

$$A = \begin{pmatrix} 0 & 0 & 1 & 1 \\ 0 & 0 & 1 & 0 \\ 1 & 1 & 0 & 0 \\ 1 & 0 & 0 & 0 \end{pmatrix}, \tag{11}$$

Now, the direction of the edges of the graph must be specified. For this purpose, $\alpha_{ij}(i \neq j)$ must be calculated according to the algorithm. After calculating α_{ij}, we will have directed algorithm $G_d(A)$. To calculate α_{ij}, the first condition is that $J_{i,i}$ must not be zero and, on the other hand, must be negative, so we apply the first controllers:

$$u = (u_1, u_2, u_3, u_4)^T = (-nx_1, -mx_2, -kx_3, -qx_4)^T \; s.t \; n > 0, m > 0, k > 0, q > 0.$$

Rewriting the Jacobian matrix by applying new controllers, we write:

$$J = \begin{pmatrix} a_1p_1 - a_1p_2x_4^2 - n & 0 & -a_1 & -2a_1p_2x_1x_4 \\ 0 & -m & -a_2 & 0 \\ -a_3 & a_3 & -k & 0 \\ -a_4 & 0 & 0 & -q \end{pmatrix}, \tag{12}$$

Now we calculate α_{ij} by applying controllers:

$$\begin{aligned} \alpha_{13} &= \tfrac{|-a_1|}{|a_1p_1 - a_1p_2x_4^2 - n|}(4-2-1), & \alpha_{31} &= \tfrac{|-a_3|}{|-k|}(4-2-1), \\ \alpha_{14} &= \tfrac{|-2a_1p_2x_1x_4|}{|a_1p_1 - a_1p_2x_4^2 - n|}(4-2-1), & \alpha_{41} &= \tfrac{|-a_4|}{|-q|}(4-3-1), \\ \alpha_{23} &= \tfrac{|-a_2|}{|-m|}(4-3-1), & \alpha_{32} &= \tfrac{|a_3|}{|-k|}(4-2-1). \end{aligned}$$

By comparing the obtained α_{ij}, we see that we have trouble calculating α_{23} and α_{41}, so we introduce the controllers as follows:

$$u = (u_1, u_2, u_3, u_4)^T = (-nx_1, -mx_2 + zx_4, -kx_3, -qx_4)^T,$$

$$s.t \quad n > 0, m > 0, z > 0, k > 0, q > 0.$$

We redefine the Jacobian matrix:

$$J = \begin{pmatrix} a_1p_1 - a_1p_2x_4^2 - n & 0 & -a_1 & -2a_1p_2x_1x_4 \\ 0 & -m & -a_2 & z \\ -a_3 & a_3 & -k & 0 \\ -a_4 & 0 & 0 & -q \end{pmatrix}, \tag{13}$$

For the Jacobian matrix, we define the adjacency matrix A and calculate α_{ij}:

$$A = \begin{pmatrix} 0 & 0 & 1 & 1 \\ 0 & 0 & 1 & 1 \\ 1 & 1 & 0 & 0 \\ 1 & 1 & 0 & 0 \end{pmatrix}, \tag{14}$$

$$\begin{aligned} \alpha_{13} &= \tfrac{|-a_1|}{|a_1p_1-a_1p_2x_4^2-n|}(4-2-1), & \alpha_{31} &= \tfrac{|-a_3|}{|-k|}(4-2-1), \\ \alpha_{14} &= \tfrac{|-2a_1p_2x_1x_4|}{|a_1p_1-a_1p_2x_4^2-n|}(4-2-1), & \alpha_{41} &= \tfrac{|-a_4|}{|-q|}(4-2-1), \\ \alpha_{23} &= \tfrac{|-a_2|}{|-m|}(4-2-1), & \alpha_{32} &= \tfrac{|a_3|}{|-k|}(4-2-1), \\ \alpha_{24} &= \tfrac{|z|}{|-m|}(4-2-1), & \alpha_{42} &= \tfrac{|0|}{|-q|}(4-2-1). \end{aligned}$$

By applying the condition $\alpha_{ij}(t,x)\alpha_{ji}(t,x) \leq 1$ the range of parameters n, m, z, k, q is determined as follows:

$$\begin{aligned} &\alpha_{13}\alpha_{31} \leq 1 \quad \rightarrow \quad k \leq 1, && \alpha_{14}\alpha_{41} \leq 1 \quad \rightarrow \quad n > a_1p_1 = 1.2375,\ q > 0, \\ &\alpha_{24}\alpha_{42} \leq 1 \quad \rightarrow \quad z < m, && \alpha_{23}\alpha_{32} \leq 1 \quad \rightarrow \quad m > 10. \end{aligned}$$

It should be noted that because α_{14} is dependent on x_1 and x_4 and the system is time-dependent, and also the direction of the edge may change with the change of time, we considered the range of q and n in such a way that the condition of being negative $J_{i,i}$ keep and no circle is formed.

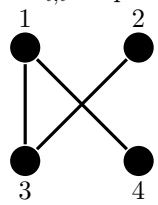

$A(11)$

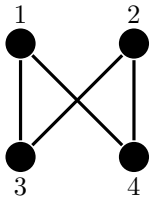

$A(14)$

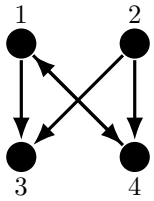

$G_d(A)$

4.2 Synchronization

Synchronization means to provide conditions so that the dynamic behavior of two similar (or different) systems with different initial conditions coincide after the passage of time. For this purpose, we consider two master and slave systems as follows:

$$\begin{cases} \dot{x} = f(x), \\ \dot{y} = f(y) + u. \end{cases} \tag{15}$$

In synchronization, u is the controller that causes two systems to be synchronized. That is mean:

$$\lim_{t\to\infty} \|y - x\| = 0.$$

To check the synchronization, we consider the system (8) as the master system and define the slave system as follows:

$$\begin{cases} \dot{y_1}(t) = a_1 p_1 y_1(t) - a_1 y_3(t) - a_1 p_2 y_1(t) y_4^2(t) + u_1, \\ \dot{y_2}(t) = -a_2 y_3(t) + u_2, \\ \dot{y_3}(t) = -a_3(y_1(t) - y_2(t)) + u_3, \\ \dot{y_4}(t) = -a_4 y_1(t) + u_4. \end{cases} \tag{16}$$

Now, we define the error system between system (8) and (16) as follows:

$$e_i = y_i - x_i, \qquad i = 1, 2, 3, 4$$

So, we have:

$$\begin{cases} \dot{e_1}(t) = a_1 p_1 e_1(t) - a_1 e_3(t) - a_1 p_2 (e_1(t) e_4^2(t) + G) + u_1, \\ \dot{e_2}(t) = -a_2 e_3(t) + u_2, \\ \dot{e_3}(t) = -a_3(e_1(t) - e_2(t)) + u_3, \\ \dot{e_4}(t) = -a_4 e_1(t) + u_4. \end{cases} \tag{17}$$

$$G = 2x_4(t)y_1(t)y_4(t) + y_1(t)x_4^2(t) - x_1(t)y_4^2(t) - 2x_1(t)x_4(t)y_4(t).$$

To obtain the system (16) controller, as in the previous section, we use the method introduced in subsection 2.2. So, we have:

$$J = \frac{\partial f}{\partial e} = \begin{pmatrix} a_1 p_1 - a_1 p_2 e_4^2 & 0 & -a_1 & -2a_1 p_2 e_1 e_4 \\ 0 & 0 & -a_2 & 0 \\ -a_3 & a_3 & 0 & 0 \\ -a_4 & 0 & 0 & 0 \end{pmatrix}, \tag{18}$$

Subsequently, the adjacency matrix is defined as follows:

$$A = \begin{pmatrix} 0 & 0 & 1 & 1 \\ 0 & 0 & 1 & 0 \\ 1 & 1 & 0 & 0 \\ 1 & 0 & 0 & 0 \end{pmatrix}. \tag{19}$$

To obtain the desired adjacency graph, we define the controller as follows:

$$\begin{cases} u_1 = -ne_1 & \rightarrow & u_1 = -n(y_1 - x_1), \\ u_2 = -me_2 + ze_4 & \rightarrow & u_2 = -m(y_2 - x_2) + z(y_4 - x_4), \\ u_3 = -ke_3 & \rightarrow & u_3 = -k(y_3 - x_3), \\ u_4 = -qe_4 & \rightarrow & u_4 = -q(y_4 - x_4). \end{cases} \tag{20}$$

We have:

$$J = \frac{\partial f}{\partial e} = \begin{pmatrix} a_1 p_1 - a_1 p_2 e_4^2 - n & 0 & -a_1 & -2a_1 p_2 e_1 e_4 \\ 0 & -m & -a_2 & z \\ -a_3 & a_3 & -k & 0 \\ -a_4 & 0 & 0 & -q \end{pmatrix}, \tag{21}$$

and

$$A = \begin{pmatrix} 0 & 0 & 1 & 1 \\ 0 & 0 & 1 & 1 \\ 1 & 1 & 0 & 0 \\ 1 & 1 & 0 & 0 \end{pmatrix}. \tag{22}$$

After obtaining the adjacency matrix, we now have to determine the graph's direction.

$$\begin{aligned} \alpha_{13} &= \tfrac{|-a_1|}{|a_1 p_1 - a_1 p_2 e_4^2 - n|}(4-2-1), & \alpha_{31} &= \tfrac{|-a_3|}{|-k|}(4-2-1), \\ \alpha_{14} &= \tfrac{|-2a_1 p_2 e_1 e_4|}{|a_1 p_1 - a_1 p_2 e_4^2 - n|}(4-2-1), & \alpha_{41} &= \tfrac{|-a_4|}{|-q|}(4-2-1), \\ \alpha_{23} &= \tfrac{|-a_2|}{|-m|}(4-2-1), & \alpha_{32} &= \tfrac{|a_3|}{|-k|}(4-2-1), \\ \alpha_{24} &= \tfrac{|z|}{|-m|}(4-2-1), & \alpha_{42} &= \tfrac{|0|}{|-q|}(4-2-1). \end{aligned}$$

To determine the direction of the graph, considering the $\alpha_{ij}(t,x)\alpha_{ji}(t,x) \leq 1$ condition, we have:

$$\begin{aligned} &\alpha_{13}\alpha_{31} \leq 1 \;\rightarrow\; k \leq 1, && \alpha_{14}\alpha_{41} \leq 1 \;\rightarrow\; n > a_1 p_1 = 1.2375,\ q > 0, \\ &\alpha_{24}\alpha_{42} \leq 1 \;\rightarrow\; z < m, && \alpha_{23}\alpha_{32} \leq 1 \;\rightarrow\; m > 10. \end{aligned}$$

Because α_{14} is dependent on e_1 and e_4 and the system is time-dependent and also the direction of the edge may change with the change of time, so the direction of the edge between the two vertices of e_1 and e_4 is considered two-way. Finally, the system controller (16) is defined as follows:

$$u = (u_1, u_2, u_3, u_4)^T = (-ne_1, -me_2 + ze_4, -ke_3, -qe_4)^T,$$

$$s.t \quad n > 1.25, m > 10, z < m, k \leq 1, q > 0.$$

4.3 Numerical simulation

In this section, we present the results obtained using the 'ode45' MATLAB software to analyze the control and synchronization operation according to the proposed controllers.

In Section 3, we showed the chaos of system (8) with parameters $a_1 = 3.75, a_2 = 10, a_3 = 1, a_4 = 1, p_1 = 0.33, p_2 = 0.25$.

Now, according to the above discussions, we define the control gain for the system (8) in Table 1:

Table 1: Controller gain.

Parameters
$n = 10$
$m = 11$
$z = 10$
$k = 1$
$q = 5$

The results are shown in Figures 9 to 11.

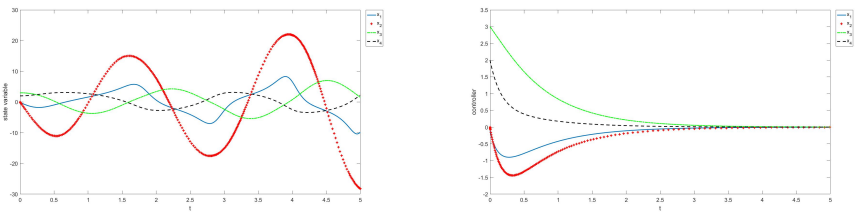

without controller with controller

Figure 9: System (8) without controller and with controller.

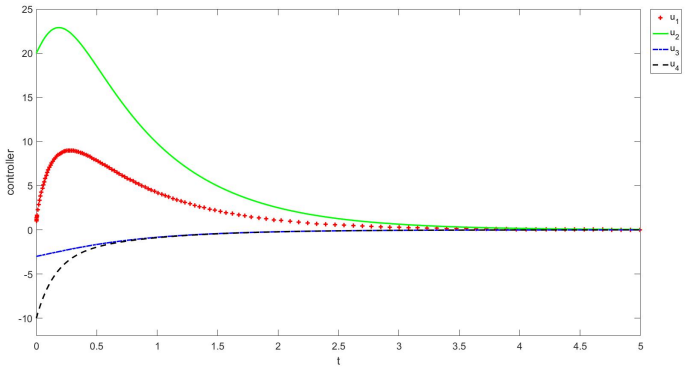

Figure 10: Designed controllers for chaotic system.

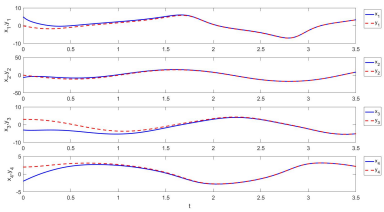

Synchronization

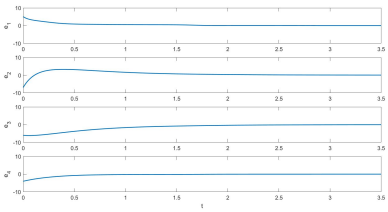

synchronization error

Figure 11: Synchronization and synchronization error of chaotic system.

5. Secure commucation

As secure communication using chaos synchronization is a crucial topic in dynamic systems, this section will focus on the encryption and decryption processes of the memristor synchronized system. In this method, we consider the transmitter system (8) with state variables $Z(t) = a_1x_1 + a_4x_4$ that produces chaotic signals as the primary system and the receiver system (16) with state variable $\hat{Z}(t) = a_1y_1 + a_4y_4$. We add the signal $M(t)$ to the chaotic carriers of the transmitter system $Z(t)$. The receiver, after receiving $M(t)+Z(t)$, subtracts the value of $\hat{Z}(t)$ from it and recovers the sent signal. The received signal is received according to the following relationship:

$$\hat{M}(t) = Z(t)_r - \hat{Z}(t) = M(t) + Z(t) - \hat{Z}(t) \simeq M(t).$$

The results are shown in Figure 12.

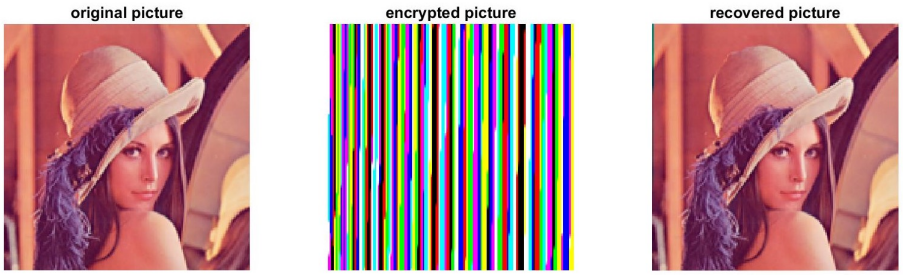

Figure 12: Secure communication based on synchronization for color digital image.

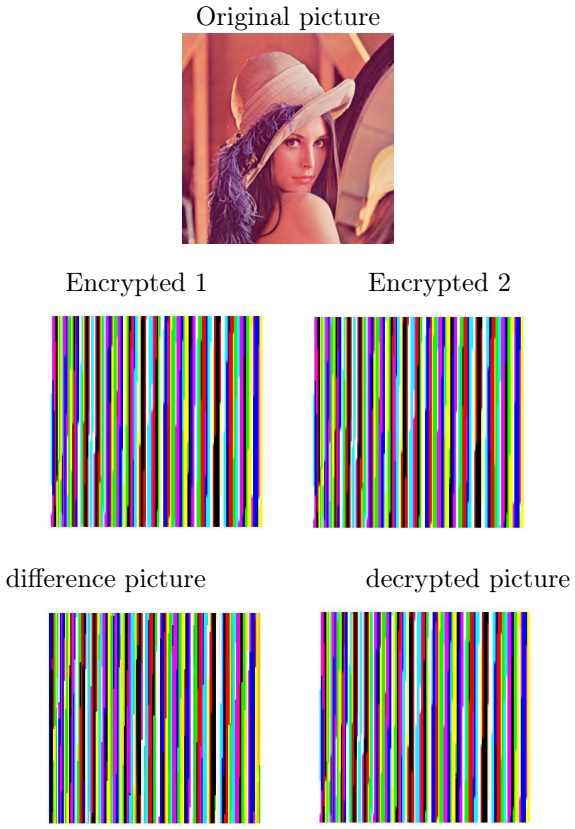

Figure 13: Key sensitivity test.

6. Security analysis

Now, to check the effectiveness of the proposed secure communication plan, we use key sensitivity analysis, statistical analysis, and speed analysis methods.

6.1 Key sensitivity analysis

In encryption, an efficient method must also be sensitive to the secret key, meaning that a minimal change in the key causes a significant change in the output. For sensitivity analysis, we change the key parameter $x_3 = 3$ to $x_3 = 3 - 10^{-3}$. We obtain the encrypted image from both modes and then we find the difference between the two encrypted images. The black pixels in the difference image between the two encoded images represent the same parts of both images. The results show that the difference ratio is significantly high, which means that the proposed

algorithm is very sensitive to key parameters. Finally, we get the decryption of the encrypted image with the parameter $x_3 = 3$ and the parameter $x_3 = 3 - 10^{-3}$. As we can see, only one correct key can decrypt an encrypted image. The sensitivity of other parameters is similar to x_3. Figure 13 shows the results of each step.

6.2 Histogram analysis

Since the image histogram is an important feature in image analysis [41, 42], in this section, we analyze the color image of Lena and the coded image statistically in RGB form. The results are shown in Figure 14. As shown in the images, the histogram of the encrypted image is relatively uniform and significantly different from the plain image. This which indicates that the encryption algorithm can effectively scatter the plain information into a random cipher and resist statistical attacks. That is, it should not provide any clues to use in a statistical analysis attack on the encrypted image.

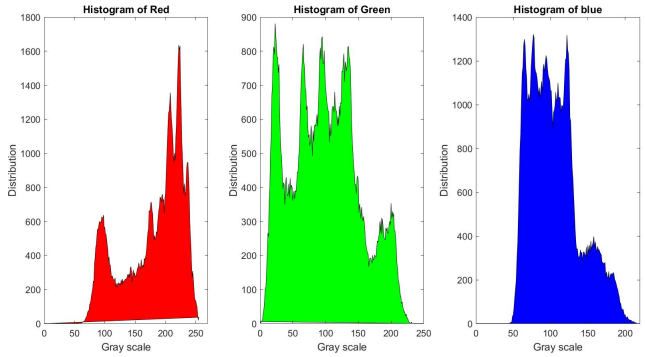

Histograms of original picture

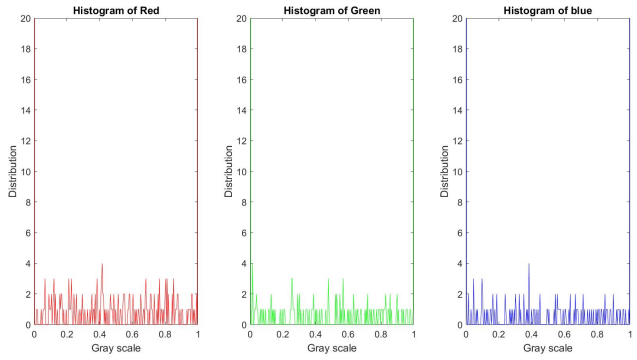

Histograms of encrypted picture

Figure 14: Histogram of the original image and encrypted image of Lena.

Table 2: Comparison of encryption time between our proposed method and another method Encryption system.

Algorithm	Encryption Time (seconds)
The proposed method	0.775459
Ref.[43]	3.704
Ref.[37]	>10
Ref.[44]	2.901
Ref.[45]	2.3

6.3 Speed analysis

Algorithm execution speed is also an important issue for an executable system. We implement the proposed algorithm using Matlab R 2016b. The speed performance has been tested on a computer with 11th Gen Intel(R) Core(TM) i5-1135G7 @ 2.40GHz processor, 7.69 GB memory, and 931.51 GB hard disk capacity and Windows 10 operating system. The parameters and algorithm of our proposed method are different from the algorithm of other methods. By comparing the results of encrypted designs in Table 2, we can see that the operation speed of our method is clearly faster for Lena's image.

7. Conclusion

In this article, the relationship between the contraction control method and the graphical algorithm method for finding the controller of chaotic systems and then synchronizing the system is stated. The behavior of the four-dimensional circuit dynamic system model based on the proposed parameter memristor has been investigated according to the initial conditions, including attractor, sensitivity, Lyapunov exponent, and bifurcation of the system. The graphical method algorithm is implemented on the memristor system for control and synchronization. The power and efficiency of the proposed method are shown by numerical simulation. Finally, Lena's color image encoding based on the chaotic system has been studied and safety performance analysis including sensitivity key analysis, histogram analysis, and speed analysis has been performed. The security analysis of the proposed overlay secure communication method shows the effectiveness of the proposed method, that is, it shows that it can be used to encrypt color images as a very secure method.

Conflicts of Interest. The authors declare that they have no conflicts of interest regarding the publication of this article.

References

[1] E. N. Lorenz, Deterministic nonperiodic flow,*J. Atmos. Sci* **20** (1963) 130 – 141.

[2] R. Femat, J. Alvarez-Ramirez, B. Castillo-Toledo and J. Gonzalez, On robust chaos suppression in a class of no driven oscillators: application to the Chua's circuit, *IEEE Trans. Circuits Syst. I* **46** (1999) 1150 – 1152.

[3] R. Femat, R. Jauregui-Ortiz and G. Solís-Perales, A chaos-based communication scheme via robust asymptotic feedback, *IEEE Trans. Circ. Syst. I* **48** (2001) 1161 – 1169.

[4] E. A. Jackson and A. Hübler, Periodic entrainment of chaotic logistic map dynamics, *Phys. D* **44** (1990) 407 – 420.

[5] E. Ott, C. Grebogi and J. A. Yorke, Controlling chaos, *Phys. Rev. Lett.* **64** (1990) #1196.

[6] M. J. Ogorzalek and Taming chaos-II: Control, *IEEE Trans. Circuits Syst. I*, **40** (1993) 700 – 706.

[7] B. B. Sharma and I. N. Kar, Contraction theory based adaptive synchronization of chaotic systems, *Chaos, Solitons & Fractals* **41** (2009) 2437 – 2447.

[8] M. T. Yassen, Controlling chaos and synchronization for the new chaotic system using linear feedback control, *Chaos Solitons Fractals* **26** (2005) 913 – 920, https://doi.org/10.1016/j.chaos.2005.01.047.

[9] W. Lohmiller and J. J. E. Slotine, On contraction analysis for nonlinear systems, *Automatica* **34** (1998) 683 – 696, https://doi.org/10.1016/S0005-1098(98)00019-3.

[10] J. P. Singh and B. K. Roy, Hidden attractors in a new complex generalized Lorenz hyperchaotic system, its synchronization using adaptive contraction theory, circuit validation and application, *Nonlinear Dyn.* **92** (2018) 373−394, https://doi.org/10.1007/s11071-018-4062-z.

[11] L. M. Pecora and T. L. Carroll, Synchronization in chaotic systems, *Phys. Rev. Lett.* **64** (1990) #821-824, https://doi.org/10.1103/PhysRevLett.64.821.

[12] M. Boutayeb, M. Darouach and H. Rafaralahy, Generalized state-space observers for chaotic synchronization with applications to secure communication, *IEEE Trans. Circuits and Systems I* **49** (2002) 345 – 349.

[13] J. Hu, S. Chen and L. Chen, Adaptive control for anti-synchronization of Chua's chaotic system, *Phys. Lett. A* **339** (2005) 455 – 460, https://doi.org/10.1016/j.physleta.2005.04.002.

[14] T. L. Liao and N. S. Huang, An observer based approach for chaotic synchronization and secure communication, *IEEE Trans. Circuits Syst. I* **46** (1999) 1144 − 1150, https://doi.org/10.1109/81.788817.

[15] B. Naderi and H. Kheiri, Exponential synchronization of chaotic system and application in secure communication, *Optik* **127** (2016) 2407 − 2412, https://doi.org/10.1016/j.ijleo.2015.11.175.

[16] B. Naderi, H. Kheiri and A. Heydari, Secure communication based on synchronization of three chaotic systems, *Int. J. Nonlinear Sci.* **27** (2019) 53−64.

[17] Y. Wang, Z. H. Guan and H. O. Wang, Feedback and adaptive control for the synchronization of Chen system via a single variable, *Phys. Lett. A* **312** (2003) 34 − 40, https://doi.org/10.1016/S0375-9601(03)00573-5.

[18] L. O. Chua, Memristor-the missing circuit element, *IEEE Trans. Circuit Theory* **18** (1971) 507 − 519.

[19] D. B. Strukov, G. S. Snider, D. R. Stewart and R. S. Williams, The missing memristor found, *Nature* **453** (2008) 80 − 83, https://doi.org/10.1038/nature06932.

[20] F. Corinto, A. Ascoli and M.Gilli, Nonlinear dynamics of memristor oscillators, *IEEE Trans. Circuits Syst. I* **58** (2011) 1323 − 1336, https://doi.org/10.1109/TCSI.2010.2097731.

[21] Z. J. Li and Y. C. Zeng, A memristor oscillator based on a twin-T network, *Chinese Phys. B* **22** (2013) #040502, https://doi.org/10.1088/1674-1056/22/4/040502.

[22] B. Bo-Cheng, L. Zhong and X. Jian-Ping, Transient chaos in smooth memristor oscillator, *Chinese Phys. B* **19** (2010) #030510, https://doi.org/10.1088/1674-1056/19/3/030510.

[23] R. K. Budhathoki, M. P. D. Sah, C. Yang, H. Kim and L. O. Chua, Transient behavior of multiple memristor circuits based on flux charge relationship, *Internat. J. Bifur. Chaos Appl. Sci. Engrg.* **24** (2014) #1430006, https://doi.org/10.1142/S0218127414300067.

[24] A. Buscarino, L. Fortuna, M. Frasca and L. V. Gambuzza, A gallery of chaotic oscillators based on HP memristor, *Internat. J. Bifur. Chaos Appl. Sci. Engrg.* **23** (2013) #1330015, https://doi.org/10.1142/S0218127413300152.

[25] R. Tetzlaff, *Memristors and Memristive Systems*, Springer New York, NY, 2013.

[26] M. E. Sahin, Z. G. Cam Taskiran, H. Guler, S. E. Hamamci, Application and modeling of a novel 4D memristive chaotic system for communication systems, *Circuits Syst. Signal Process* **39** (2020) 3320 – 3349, https://doi.org/10.1007/s00034-019-01332-6.

[27] X. Wu, S. He, W. Tan and H. Wang, From memristor-modeled jerk system to the nonlinear systems with memristor, *Symmetry* **14** (2022) #659, https://doi.org/10.3390/sym14040659.

[28] G. Russo and M. di Bernardo, An algorithm for the construction of synthetic self synchronizing biological circuits, *In International Symposium on Circuits and Systems* (2009) 305 – 308, https://doi.org/10.1109/ISCAS.2009.5117746.

[29] S. Sabarathinam, V. Papov, Z. P. Wang, R. Vadivel and A. P. P. A. N Gunasekaran, Dynamics analysis and fractional-order nonlinearity system via memristor-based Chua oscillator, *Pramana* **97** (2023) #107, https://doi.org/10.1007/s12043-023-02590-5.

[30] W. Lohmiller and J. J. E Slotine, Control system design for mechanical systems using contraction theory, *IEEE Trans. Automat. Control* **45** (2000) 984 – 989, https://doi.org/10.1109/9.855568.

[31] J. P. Singh, S. Jafari, A. J. M. Khalaf, V-T Pham and B. K. Roy, A modified chaotic oscillator with megastability and variable boosting and its synchronisation using contraction theory-based control which is better than backstepping and nonlinear active control, *Pramana* **94** (2020) 1 – 14, https://doi.org/10.1007/s12043-020-01993-y.

[32] X. Zhang and B. Cui, Synchronization of Lurie system based on contraction analysis, *Appl. Math. Comput.* **223** (2013) 180 – 190, https://doi.org/10.1016/j.amc.2013.07.080.

[33] G. Russo, *Analysis, Control and Synchronization of Nonlinear Systems and Networks via Contraction Theory: Theory and Applications* Ph.D. Thesis, Department of Systems and Computer Engineering University of Naples Federico II, Napoli, Italy 2010.

[34] B. B. Sharma and I. N. Kar, Observer-based synchronization scheme for a class of chaotic systems using contraction theory, *Nonlinear Dyn* **63** (2011) 429 – 445, https://doi.org/10.1007/s11071-010-9813-4.

[35] L. Ren, J. Mou, H. Jahanshahi, A. A. Al-Barakati and Y. Cao, A new multistable chaotic system with memristor and memcapacitor for fractional-order: dynamical analysis, implementation, and synchronization, *Eur. Phys. J. Plus* **138** (2023) 1 – 20, https://doi.org/10.1140/epjp/s13360-023-04379-2.

[36] G. Russo, M. di Bernardo and J. J. E. Slotine, A graphical algorithm to prove contraction of nonlinear circuits and systems, *IEEE Transactions on Circuits and Systems I* **58** (2011) 336 − 348, https://doi.org/10.1109/TCSI.2010.2071810.

[37] Y. Ruisong, A novel chaos-based image encryption scheme with an efficient permutation-diffusion mechanism, *Opt. Commun.* **284** (2011) 5290 − 5298, https://doi.org/10.1016/j.optcom.2011.07.070.

[38] M. di Bernardo, G. Russo and J. J. Slotine, An algorithm to prove contraction, consensus, and network synchronization, *In Proceedings of the International Workshop NecSys* **42** (2009) 60 − 65, https://doi.org/10.3182/20090924-3-IT-4005.00011.

[39] C. Godsil and G. Royle, *Algebraic Graph Theory*, Springer-Verlag New York, Inc. 2001.

[40] H. Sayama, *Introduction to the Modeling and Analysis of Complex Systems*, Open SUNY Textbooks, 2015.

[41] C. K. Volos, I. M. Kyprianidis and I. N. Stouboulos, Image encryption process based on chaotic synchronization phenomena, *Signal Process.* **93** (2013) 1328 − 1340, https://doi.org/10.1016/j.sigpro.2012.11.008.

[42] Y. Xu, H. Wang, Y. Li and B. Pei, Image encryption based on synchronization of fractional chaotic systems, *Commun. Nonlinear Sci. Numer. Simul.* **19** (2014) 3735 − 3744, https://doi.org/10.1016/j.cnsns.2014.02.029.

[43] S. Lian, J. Sun and Z. Wang, A block cipher based on a suitable use of chaotic standard map, *Chaos, Solitons & Fractals* **26** (2005) 117 − 129, https://doi.org/10.1016/j.chaos.2004.11.096.

[44] A. H. Abdullah, R. Enayatifar and M. Lee, A hybrid genetic algorithm and chaotic function model for image encryption, *AEU–Int. J. Electron. Commun.* **66** (2012) 806 − 816, https://doi.org/10.1016/j.aeue.2012.01.015.

[45] G. Ye, Image scrambling encryption algorithm of pixel bit based on chaos map, *Pattern Recognit. Lett.* **31** (2010) 347 − 354, https://doi.org/10.1016/j.patrec.2009.11.008.

Marzieh Pabasteh
Department of Mathematics,
Payame Noor University, (PNU),
Tehran, I. R. Iran
e-mail: M.Pabasteh@yahoo.com

Bashir Naderi
Department of Mathematics,
Payame Noor University,(PNU),
Tehran, I. R. Iran
e-mail: b_naderi@pnu.ac.ir